Learned Templates for Feature Extraction in Fingerprint Images

Bir Bhanu and Xuejun Tan
Center for Research in Intelligent Systems
University of California, Riverside, CA92521, USA
Email: {bhanu, xtan}@cris.ucr.edu

Abstract

Most current techniques for minutiae extraction in fingerprint images utilize complex preprocessing and postprocessing. In this paper, we propose a new technique, based on the use of learned templates, which statistically characterize the minutiae. Templates are learned from examples by optimizing a criterion function using Lagrange's method. To detect the presence of minutiae in test images, templates are applied with appropriate orientations to the binary image only at selected potential minutia locations. Several performance measures, which evaluate the quality and quantity of extracted features and their impact on identification, are used to evaluate the significance of learned templates. The performance of the proposed approach is evaluated on two sets of fingerprint images: one is collected by an optical scanner and the other one is chosen from NIST special fingerprint database 4. The experimental results show that learned templates can improve both the features and the performance of the identification system.

1 Introduction

In most automatic fingerprint identification systems, minutiae, including endpoints and bifurcations, are commonly used as features. However, reliable minutiae extraction in fingerprint images is still a difficult problem. This problem is complicated by the fact that fingerprint images can be substantially distorted due to noise, scars and undesired artifacts.

A minutiae extraction approach generally consists of three steps: preprocessing, feature extraction and postprocessing. Preprocessing techniques attempt to utilize the nature of fingerprint images for image filtering, which is adaptive to local orientation and local frequency [1,2,3]. Feature extraction is based on either binarization, thinning and minutiae detection, or a ridge following approach in either binary or gray scale images [4,5]. The approaches based on binarization, thinning and minutiaedetection are simple in principle, and some of the algorithms, like thinning, can be implemented in parallel. However, they tend to perform poorly in noisy and low contrast images. In comparison, ridge following approaches have the advantage that they can perform better on noisy and low contrast images. However, the algorithms are generally complex and nonadaptive. Postprocessing techniques attempt to rectify imperfections of the feature extraction by utilizing model information such as minimum ridge length and the duality between ridges and valleys. Table 1 shows some techniques for minutiae purification. Generally, these algorithms are complex and heavily depend on the experimental parameters.

A minutiae extraction algorithm has been proposed [6] which uses fixed templates. The assumptions in using fixed templates are: a) ridge width is constant in a fingerprint image; b) minutiae are not located in an area where the local orientation changes rapidly. However, in reality, ridge width is not always constant, and local orientation changes rapidly in certain areas, such as around the delta and core points. Motivated to develop a distortion tolerant approach that can deal with these problems and be computationally efficient, in this paper we present a template based approach for minutiae extraction, which is based on learning templates by Lagrange's method. The key contributions of this paper are the development of a new technique for learning templates for endpoints and bifurcations from examples and applying them adaptively to extract minutiae in fingerprints. The results are evaluated using several measures on two different datasets to demonstrate the efficacy of the technique.

2 Learned minutiae extraction

Figure 1 shows the block diagram of our system. First, the background (area with no information) in the fingerprint image is removed. Local orientation is computed in each local block and the fingerprint is adaptively smoothed according to the local orientation. Then, the fingerprint is adaptively binarized and thinned. Potential minutiae are found using Crossing Number (*CN*). Finally, learned templates are adaptively applied to purify the potential minutiae.

0-7695-1272-0/01 $10.00 © 2001 IEEE

Table 1. Techniques for minutiae purification.

System	Processing	Approach	Evaluation	Comments
Xiao et al., 1991, [7]	Postprocessing to purify minutiae	Statistical criteria	Reduction of false minutiae	8 algorithms to filter false minutiae
Sherlock et al., 1994, [2]	Preprocessing for enhancement of gray-scale image	Directional Fourier filtering	# of missed minutiae and false minutiae	Results were checked on only 14 images
Hong et al., 1998, [1]	Preprocessing for enhancement of gray-scale image	Gabor filter adaptive to local orientation	Goodness Index and verification performance	Computationally expensive and too many parameters
Farina et al., 1999, [8]	Postprocessing to purify minutiae	Knowledge based criteria	Visual check	9 algorithms to filter false minutiae
Luo et al., 2000, [9]	Postprocssing to purify minutiae	Knowledge based criteria	N/A	Too many rules and parameters
This paper	Apply templates to filter minutiae	Learned templates based on criteria	Goodness Value, *ROC* curve and identification performance	

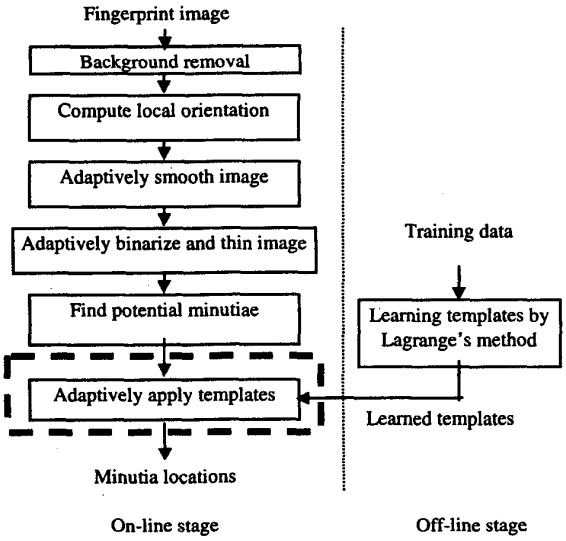

Figure 1. System for minutiae extraction.

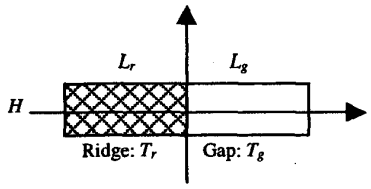

Figure 2. Illustration of an ideal endpoint template T.

2.1 Off-line learning of templates

• **Template learning problem:** A template is a 2D filter that is concerned with detecting a minutia. Since a minutia can be an endpoint or a bifurcation, two templates are to be learned, one for each kind of feature. For simplicity, we use endpoints as the example to explain our learning approach. The template for bifurcations can be learned by following a similar processing.

Figure 2 shows an ideal endpoint template T that consists of two sub-templates, T_r (length L_r) and T_g (length L_g), which denote the template for ridge and gap, respectively. For simplicity, we assume $L_r = L_g$. H and L are the height and the length of the template T, and $L = L_r + L_g$. The value of each pixel in T_r and T_g are 1 and 0, respectively.

Suppose a) a ridge end E in a binary image is as ideal as the ideal template T; b) the local orientation at the ridge end is θ_i; c) the correlations between the template T and the ideal ridge end E with the orientation θ_i and $\theta_i + \pi$ are f_{θ_i} and $f_{\theta_i+\pi}$, respectively; and d) the difference between f_{θ_i} and $f_{\theta_i+\pi}$ is Δ_{θ_i}, then

$$\Delta_{\theta_i} = f_{\theta_i} - f_{\theta_i+\pi} \quad (1)$$

The correlation between a template T and a ridge end E with the orientation θ_i is defined by:

$$f_{\theta_i} = \sum_{(h,l)\in(T\cap E_{\theta_i})} \{ T(h,l)\times E_{\theta_i}(h,l) \} \quad (2)$$

where $E_{\theta_i}(h, l)$ is the ridge with orientation θ_i and the template is applied along the ridge.

Under real-world conditions, the ridge end in a fingerprint image is not ideal, so that the weight of each pixel in the template cannot be measured by 1 or 0 alone. The problem of learning templates for minutiae extraction is described as: given examples of endpoints and bifurcations, how to learn the templates that can be applied to minutiae extraction to avoid the complex postprocessing?

• **Training data:** Suppose a) the examples of endpoints and bifurcations are obtained from M fingerprint images FI_k, where $k = 1,2,3...M$; b) in the kth fingerprint image FI_k, there are N_k feature locations $(x_{k,i}, y_{k,i})$, where $i = 1,2,3...N_k$; c) in the local area around $(x_{k,i}, y_{k,i})$, $I_{k,i}(m, n)$ is the gray scale value at pixel (m, n) of the image FI_k, where $x_{k,i} - d_1 \le m \le x_{k,i} + d_1$, $y_{k,i} - d_2 \le n \le y_{k,i} + d_2$, d_1 and d_2 are constants; and d) $G = \{(x_{k,i}, y_{k,i})\}$. For each pixel in G, we do the following steps: a) estimate the local orientation $\theta_{k,i}$ at pixel $(x_{k,i}, y_{k,i})$ in the local area; b) adaptively smooth $I_{k,i}(m, n)$ in the local area; c) adaptively binarize $I_{k,i}(m, n)$ in the local area.

• **Optimzation for templates learning:** Suppose a) the template is $T(h, l)$, where $1 \le h \le H$, $1 \le l \le L$, and $H = 2d_1 + 1$ and $L = 2d_2 + 1$; b) $B_{k,i}(h, l)$ is the binary image of $I_{k,i}(m, n)$; and c) $B^{\theta_{k,i}}_{k,i}(h, l)$ is the rotated binary image of $B_{k,i}(h, l)$, rotation angle is $\theta_{k,i}$, which is the local orientation at pixel $(x_{k,i}, y_{k,i})$. According to equations (1) and (2), the objective of the learning algorithm can be defined as:

$$\arg\max_{T}\left\{ \sum_{k=1}^{M}\sum_{i=1}^{N_k}\sum_{h=1}^{H}\sum_{l=1}^{L}\left[T(h,l) \times Q_{k,i}(h,l) \right] \right\} \quad (3)$$

where

$$Q_{k,i}(h,l) = B^{\theta_{k,i}}{}_{k,i}(h,l) - B^{\theta_{k,i}}{}_{k,i}(h,L-l) \quad (4)$$

If we normalize the template so that its energy is 1,

$$\sum_{h=1}^{H}\sum_{l=1}^{L} T^2(h,l) = 1 \quad (5)$$

Then, we can solve the optimization problem with Lagrange's method. Let

$$q(h,l) = \sum_{k=1}^{M}\sum_{i=1}^{N_k} Q_{k,i}(h,l) \quad (6)$$

$$\gamma = \sum_{h=1}^{H}\sum_{l=1}^{L}[T(h,l)\times q(h,l)] + \lambda\left[\sum_{h=1}^{H}\sum_{l=1}^{L} T^2(h,l) - 1\right] \quad (7)$$

Then, we have

$$\frac{\partial \gamma}{\partial T(h,l)} = q(h,l) + 2\lambda \times T(h,l) \quad (8)$$

Let

$$\frac{\partial \gamma}{\partial T(h,l)} = 0 \quad (9)$$

Then, the solution of equation (7) is,

$$\lambda = \frac{-\sqrt{\sum_{h=1}^{H}\sum_{l=1}^{L} q^2(h,l)}}{2} \quad (10)$$

And

$$T(h,l) = \frac{q(h,l)}{\sqrt{\sum_{h=1}^{H}\sum_{l=1}^{L} q^2(h,l)}} \quad (11)$$

2.2 Run time feature extraction: As shown in Figure 1, the proposed approach consists of six steps: background removal, compute local orientation, adaptively smooth image, adaptively binarize and thin image, find potential minutiae and minutiae extraction by adaptively applying templates. The detail of these steps can be found in [6].

Figure 3. Typical images in dataset 1.

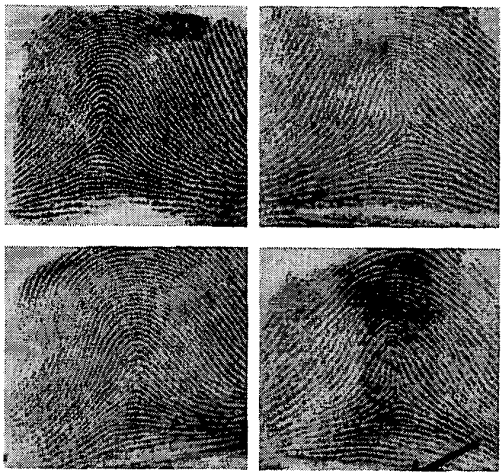

Figure 4. Typical images in dataset 2.

3 Experiments

3.1 Database: Two sets of fingerprint images are used in our experiments. Dataset 1 consists of 400 pairs of images. These images are collected from 100 persons

under real-world conditions by a commercially available optical fingerprint sensor (FIU-500-F01) with the resolution of 300 DPI. The size of these images is 248×120 pixels. We subjectively classify the 400 pairs of images according to their quality into three classes: good, fair and poor. The quality of each pair of images is determined visually based on the following criteria: contrast between ridges and valleys, ridges' continuity and width, distance between ridges, the number of scars, translation, rotation and scale between images. Some typical images from each class are shown in Figure 3. Note that the composition of dataset 1 for good, fair, and poor quality images are 19.0%, 33.2%, and 47.8%, respectively. Dataset 2 contains 400 pairs of images chosen from NIST special fingerprint database 4 (NIST-4) [10]. NIST-4 is a difficult fingerprint database in which fingerprint images are captured by an ink based method and they are not of good quality. We choose 400 pairs of images from the first 1000 pairs of images in NIST-4. These images are chosen visually based on the size of overlapped areas between two images, the number of scars, translation, rotation and scale between images. The size of these images is 480×512 pixels with the resolution of 500 DPI. Some typical images in NIST-4 that we use are shown in Figure 4.

(a) dataset 1

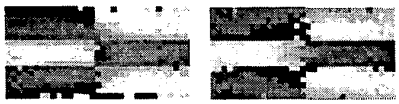

(b) dataset 2

Figure 5. Learned templates: endpoint (left) and bifurcation (right).

3.2 Learned templates: The training data is randomly and manually obtained from 30 fingerprint images in both datasets based on the quality and the location of the minutiae. There are 92 endpoints and 83 bifurcations for dataset 1, and 85 endpoints and 86 bifurcations for dataset 2. The templates for endpoint and bifurcation are learned from these training data by the procedure described in Section 2. Figure 5 shows the learned templates, which are used to extract minutiae, for each dataset. The size of the templates are 11x17 and 17x33 for two datasets, respectively. Note that, in order to show the structure of the templates clearly, the templates are normalized such that the minimum and maximum values map to black (0) and white (1), respectively.

3.3 Evaluation of experimental results: Figure 6 shows an example of minutiae extraction for each class in dataset 1 and two examples for dataset 2. The minutiae in black areas on the border of images in dataset 1 are ignored since in these areas the error in estimating local orientation is large.

- **Evaluation using the number of extracted features:** Suppose $M_e = \{e_i, i = 1,2,3...n\}$ is the set of n minutiae extracted by a feature extraction algorithm and $M_g = \{g_j, j = 1,2,3...m\}$ is the set of m minutiae extracted by an expert in a fingerprint. We define the following terms: a) *Matched* minutiae: if minutia e_i is located in an uncertainty region centered around minutia g_j, e_i and g_j are matched minutiae; b) *Occluded* minutia: if minutia g_j is not in an uncertainty region of any minutia e_i, then g_j is an occluded minutia; c) *Clutter* minutia: if e_i is not in an uncertainty region of any minutia g_j, then e_i is a clutter minutia. In our experiments, the size of the uncertainty region is 4×4 and 8×8 for dataset 1 and dataset 2, respectively. The Goodness Value (*GV*) of extracted feature is defined as:

$$GV = \frac{n_m}{n_m + n_o + n_c} \tag{12}$$

where n_m, n_o and n_c are the number of matched, occluded and clutter minutiae, respectively.

Figure 7 shows the Goodness Value of five images in each class of dataset 1 and fifteen images in dataset 2. From these figures, we find that the learned templates work better than the fixed templates described in [6]. For example, in dataset 2, the mean of *GV* on these fifteen images is 0.66 for the learned templates, and 0.57 for the fixed templates, which amounts to an improvement of 15.7%.

- **Evaluation using *ROC* curve:** By varying the decision threshold, we obtain a form of Receiver Operating Characteristic (*ROC*) curve with probability of correct feature extraction P_c vs. probability of false alarm P_f, where P_c and P_f are defined as:

$$P_c = P\{\text{decide true minutia} \mid \text{the potential minutia is a true minutia}\},$$
$$P_f = P\{\text{decide true minutia} \mid \text{the potential minutia is not a true minutia}\} \tag{13}$$

Figure 8 shows the *ROC* curve on both datasets using the learned templates. We find that the learned templates are more effective on endpoint extraction than bifurcation.

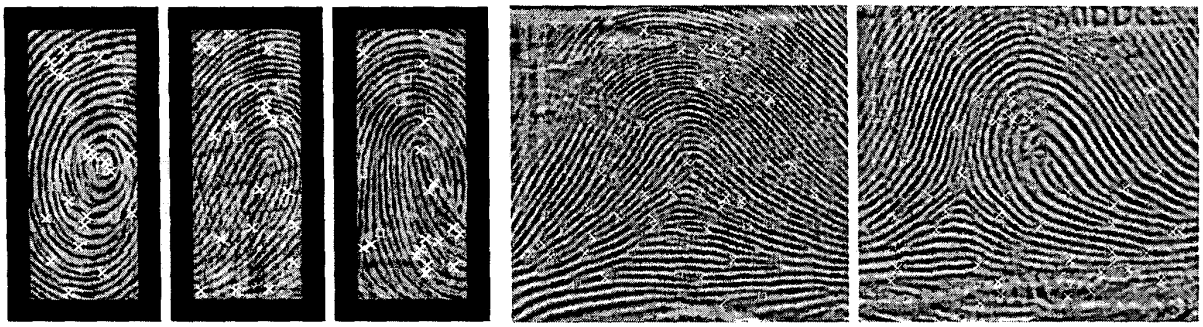

(a) dataset 1 (good, fair and poor quality) (b) dataset 2

Figure 6. Examples of minutiae extraction (□: endpoint, ×: birfucation).

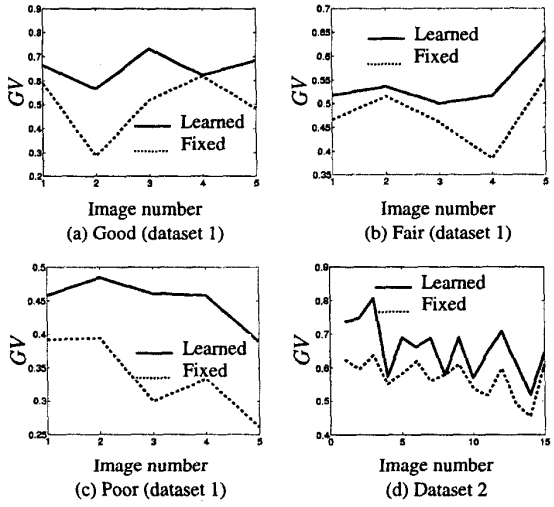

Figure 7. Goodness Value in each class on dataset 1 and on dataset 2.

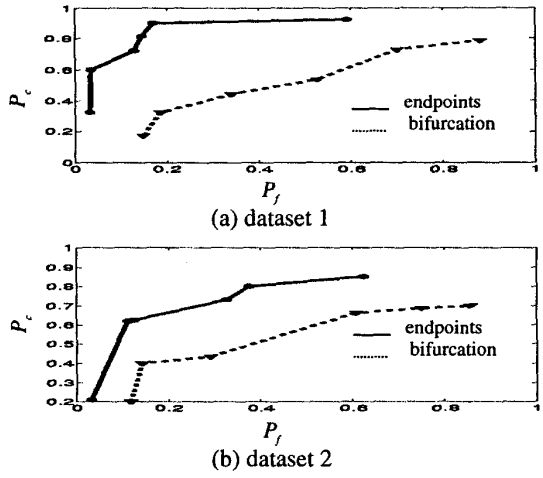

Figure 8. *ROC* curve of experiment results.

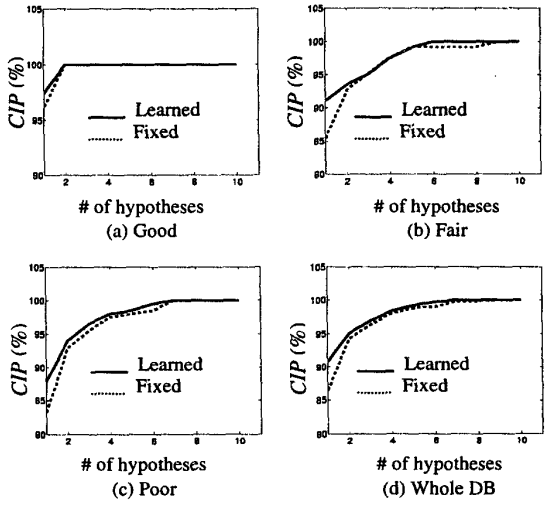

Figure 9. The comparison of indexing experimental results on dataset 1.

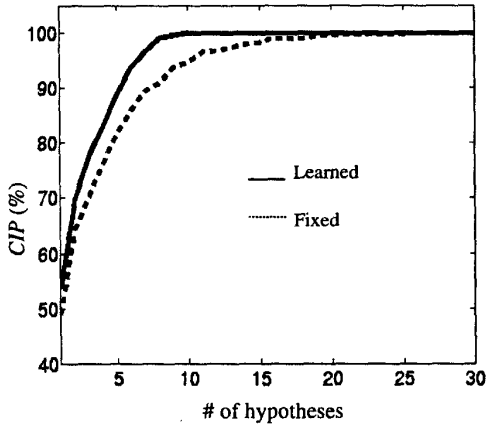

Figure 10. The comparison of indexing experimental results on dataset 2.

• **Evaluation by identification performance:** An indexing algorithm for recognition of fingerprints is presented in [11]. The outputs of the indexing algorithm are the top N hypotheses which is different from the single output of a conventional verification system. Generally, False Accept Rate (*FAR*) and False Reject Rate (*FRR*) are used to evaluate the performance of a verification algorithm. Since the output of the indexing algorithm are the top N hypotheses, *FAR* and *FRR* are not suitable for evaluating the results of an indexing algorithm. A test image, which has a corresponding image in the database, is said to be correctly indexed if it has enough corresponding entities in the model database and the correct corresponding image appears in a shortlist of hypotheses obtained by the indexing approach. Thus, the Correct Index Power (*CIP*) is defined as:

$$CIP = \frac{N_{ci}}{N_d} \times 100\% \qquad (14)$$

where N_{ci} is the number of correctly indexed images, N_d is the number of images in the database, and all images in the database are tested once by the corresponding test images.

Figure 9 and 10 show the comparison of the *CIP* for fixed and learned templates on dataset 1 and dataset 2, respectively. We observe that the performance of the learned templates is always better than that of the fixed templates. For dataset 1, the *CIP* is improved by 1.2%, 5.6%, and 4.6% for the top one hypothesis for good, fair, and poor classes, respectively. For the entire dataset 1, the *CIP* is improved by 4.3%. For dataset 2, the *CIP* for the top one hypothesis increases by 2.8%, and by 6.5% and 5.2% when we consider the top five and top ten hypotheses, respectively. Using the fixed templates, the *CIP* reaches 100% only when we consider the top twenty-six hypotheses. While for learned templates, we only need to consider top ten hypotheses. There is a difference in results on the two datasets. This is because for dataset 1 the scanner constraints the range of the distortions, while for dataset 2 there are no such constrains. And for dataset 2, since fingerprint images are collected by ink, the distortions created by blurred areas are much more than that in dataset 1.

4 Conclusions

We have proposed a new and effective fingerprint minutiae extraction algorithm which is based on using *learned templates*. Using this algorithm, we can avoid the complex preprocessing and postprocessing algorithms which are necessary in most minutiae extraction algorithms. The performance of the algorithm is evaluated by the Goodness Value on typical images, *ROC* curve on two datasets, and the performance of indexing of an identification system. Experimental results show that our minutiae extraction algorithm is capable of improving both the Goodness Value and the performance of the identification system.

Acknowledgment: This work is supported in part by a grant from Sony, DiMI and I/O software. The contents and information do not necessarily reflect the positions or policies of the sponsors.

References

[1] L. Hong, Y. Wan and A.K. Jain, Fingerprint image enhancement: algorithm and performance evaluation, IEEE Trans. on Pattern Analysis and Machine Intelligence, Vol. 20, No. 8, pp. 777-789, 1998.

[2] B.G. Sherlock, D.M. Monro and K. Millard, Fingerprint enhancement by directional Fourier filtering, IEE Proc. on Vision, Image and Signal Processing, Vol. 141, No. 2, pp. 87-94, April 1994.

[3] B.M. Mehtre, Fingerprint image analysis for automatic identification, Machine Vision and Applications, Vol. 6, No. 2-3, pp. 124-139, Spring-Summer 1993.

[4] D. Mario and D. Maltoni, Direct gray-scale minutiae detection in fingerprints, IEEE Trans. on Pattern Analysis and Machine Intelligence, Vol. 19, No. 1, pp. 27-40, 1997.

[5] X. Jiang, W.Y. Yau and W. Ser, Detecting the fingerprint minutiae by adaptive tracing the gray-level ridge, Pattern Recognition, Vol. 34, No. 5, pp. 999-1013, 2001.

[6] B. Bhanu, M. Boshra and X. Tan, Logical templates for feature extraction in fingerprint images, Proc. Int. Conf. on Pattern Recognition, Vol. 3, pp. 850-854, 2000.

[7] Q. Xiao and H. Raafat, Fingerprint image postprocessing: a combined statistical and structural approach, Pattern Recognition, Vol. 24, No. 10, pp. 985-992, 1991.

[8] A. Farina, Z.M. Kovacs-Vajna and A. Leone, Fingerprint minutiae extraction from skeletonized binary images, Pattern Recognition, Vol. 32, No. 5, pp. 877-889, 1999.

[9] X.P. Luo and J. Tian, Knowledge based fingerprint image enhancement, Proc. Int. Conf. on Pattern Recognition, Vol. 3, pp. 783-786, 2000.

[10] C.I. Watson and C.L. Wilson, NIST special database 4: fingerprint database, National Institute of Standards and Technology, March, 1992.

[11] B. Bhanu and X. Tan, A triplet based approach for indexing of fingerprint database for identification, Proc. Int. Conf. on Audio- and Video-Based Biometric Person Authentication, pp. 205-210, 2001.